

Geophysical Research Letters

RESEARCH LETTER

10.1029/2020GL090238

Key Points:

- Southeast Australian droughts are driven by circulation anomalies that reduce moisture inflow and a lack of precipitation-generating mechanisms
- Moisture for drought termination is typically sourced from the Tasman and Coral Seas
- Land surface moisture sources amplify drought by up to 6%, minor compared to ocean influence

Supporting Information:

- Supporting Information S1

Correspondence to:

C. M. Holgate,
chiara.holgate@anu.edu.au

Citation:

Holgate, C. M., Van Dijk, A. I. J. M., Evans, J. P., & Pitman, A. J. (2020). Local and remote drivers of southeast Australian drought. *Geophysical Research Letters*, 47, e2020GL090238. <https://doi.org/10.1029/2020GL090238>

Received 10 AUG 2020

Accepted 3 SEP 2020

Accepted article online 9 SEP 2020

Local and Remote Drivers of Southeast Australian Drought

C. M. Holgate^{1,2} , A. I. J. M. Van Dijk¹ , J. P. Evans^{3,4} , and A. J. Pitman^{3,4} 

¹Fenner School of Environment and Society, Australian National University, Canberra, ACT, Australia, ²ARC Centre of Excellence for Climate System Science, UNSW, Sydney, New South Wales, Australia, ³ARC Centre of Excellence for Climate Extremes, UNSW, Sydney, New South Wales, Australia, ⁴Climate Change Research Centre, UNSW, Sydney, New South Wales, Australia

Abstract Droughts are associated with large-scale modes of variability, synoptic-scale systems, and terrestrial processes. Quantifying their relative roles in influencing drought guides process understanding, helps identify weaknesses in climate models, and focuses model improvements. Using a Lagrangian back-trajectory approach we provide the first quantification of the change in moisture supply during major droughts in southeast Australia, including the causes of the changes. Drought onset and intensification were driven by reduced moisture supply from the ocean, as moisture was circulated away from the region, combined with an absence of precipitation-generating mechanisms over land. During termination, strengthened moist easterly flows from the Tasman and Coral Seas promoted anomalously high rainfall. Our approach reveals terrestrial moisture sources played a secondary role, amplifying rainfall anomalies by less than 6%. Simulating droughts therefore requires deeper understanding of the relationship between moisture advection and synoptic-scale circulation and how large-scale climate variability and terrestrial processes modify these relationships.

Plain Language Summary The relative roles of atmospheric circulation, weather systems, and land surface processes in recurring droughts in southeast Australia are unclear. We tracked the path of moisture as it moved through the air to find where the rain in southeast Australia comes from and what was different in the atmosphere and land surface during the development, deepening and breaking of three major droughts. We found that the leading cause for drought was that moisture originating from the oceans did not reach the Murray-Darling Basin as often and produced less rain when it did. The drying landscape exacerbated the low rainfall conditions but had a smaller effect than the ocean. The droughts were broken by strong systems from the east carrying moisture from the ocean into the region. To better model and predict drought we therefore need to understand the relationship between ocean moisture and the weather systems that transport it to the land and how the relationship is affected by the land surface and variability within the climate.

1. Introduction

The Millennium Drought (2001–2009) was the longest drought in the instrumental record (Van Dijk et al., 2013) whereas the subsequent, most recent drought (2017–2020) has been the most severe. The impact of drought is exacerbated by global warming such that 2019 was the warmest and driest year on record (Bureau of Meteorology, 2020a). The recent hot and dry conditions contributed to an unprecedented bush-fire season (Boer et al., 2020) and a serious health emergency (Yu et al., 2020). Low inflows led to record low volumes in water storages (Murray-Darling Basin Authority, 2020). One region in southeast Australia particularly susceptible to drought is the Murray-Darling Basin (MDB), where the long-term trend to warmer and drier conditions has affected the profitability of agriculture significantly (Hughes et al., 2019).

Drought in the MDB is associated with large-scale modes of variability. Rainfall variability and periods of above- and below-average rainfall have been linked with the El Niño-La Niña cycle (e.g., Chiew et al., 1998), the Indian Ocean Dipole (e.g., Ashok et al., 2003), the Southern Annular Mode (e.g., Hendon et al., 2007), the Interdecadal Pacific Oscillation (e.g., Power et al., 1999), and combinations of each (e.g., Ummenhofer et al., 2010). These modes of variability act to modify the probability of rainfall over southeast Australia by perturbing the large-scale circulation of the atmosphere and the frequency and location of rain-bearing

synoptic-scale systems. However, the direct, physical processes that drive the onset, intensification, and termination of southeast Australian droughts are not well understood. Anomalously low rainfall can be due to changes in moisture supply from typical evaporative source regions, either via a reduction in evaporation or due to anomalous atmospheric circulation patterns redirecting the moisture elsewhere. Using a Lagrangian back-trajectory approach, we establish the cause of altered atmospheric moisture supply for rainfall during meteorological drought onset, intensification, and termination in southeast Australia. While large-scale modes of variability and interactions with synoptic-scale systems play a role, some contribution from terrestrial processes is also likely. Our approach combines information on moisture sources, circulation change, and land-atmosphere feedbacks across individual stages of drought, building on previous studies of moisture transport variability (e.g., Bosilovich & Chern, 2006; Dirmeyer & Brubaker, 1999; Drumond et al., 2017; Gimeno et al., 2010; Herrera-Estrada et al., 2019; Miralles et al., 2016; Roy et al., 2019; Stojanovic et al., 2017; Van Der Ent et al., 2010; Wei et al., 2016). Our approach can be applied anywhere in the world to establish the cause of modified atmospheric moisture supply, establish whether land processes amplify or dampen rainfall anomalies, and in doing so establish the relative roles of local and remote processes influencing the different stages of drought.

While some progress has been made to understand the role of terrestrial processes during drought (Herrera-Estrada et al., 2019; Roundy et al., 2013; Roy et al., 2019; Zeng et al., 2019; Zhou et al., 2019), for many regions of the world, including southeast Australia, it is uncertain whether local land-atmosphere feedbacks act to amplify or suppress atmospheric moisture during drought. Here, we quantify the amplification of rainfall anomalies by the land surface as droughts intensify and terminate and the relative roles of local and remote processes influencing each drought stage. Proper representation of land-atmosphere feedbacks is essential for realistic drought simulation (Schubert et al., 2016). Our analysis is therefore central to resolving why climate models struggle to simulate droughts well (Ukkola et al., 2018) and helps provide a means to establish whether climate models simulate droughts for the right reasons.

2. Materials and Methods

2.1. Back-Trajectory Model

We estimated the evaporative origin of the moisture for rainfall falling in the northern and southern regions of the MDB with a three-dimensional (3D) Lagrangian back-trajectory model. The model was based on Dirmeyer and Brubaker (1999), but in addition to water vapor we also tracked other forms of atmospheric water (liquid and solid). Moisture supplying rainfall events of $>2 \text{ mm d}^{-1}$ between 1979 and 2013 were tracked. For each day rainfall occurred within a grid cell, moist air parcels were launched from a precipitable water-weighted height in the atmosphere at a rate proportional to the rainfall rate and advected through the atmosphere using 3-D wind fields. As parcels moved across the grid at each 10-minute back-trajectory time step, a proportion of the parcel's moisture was assumed to come from evaporation from the Earth's surface below the parcel at that point in its trajectory. Parcels were tracked until (i) all the precipitable water at the original rain cell was accounted for, (ii) the parcel reached the edge of the model domain (Figure 1a), or (iii) the maximum back-trajectory time (30 days) was reached. The algorithm provided daily maps of evaporated water that contributed to rainfall over the MDB every day during the 35-year time frame. Anomalies of moisture supply to the MDB during droughts were then calculated as deviations from the 35-year climatology.

The back-trajectory model was forced with 3D, six-hourly, 0.5° atmospheric fields of wind, temperature, precipitable water and pressure, and 2-D fields of rainfall and surface fluxes. Atmospheric fields were simulated using the ERA-Interim-driven WRFv3.6.1 simulation. The simulation was spectrally nudged with winds and geopotential height above approximately 500 hPa using ERA-Interim to ensure synoptic-scale systems remained close to the reanalysis. The WRF simulation performed well against observations of temperature and rainfall and was deemed suitable for the purposes of this study. For further detail of the evaluation and back-trajectory model, the reader is directed to Holgate et al. (2020).

2.2. Definition of Drought Stages

The Bureau of Meteorology (2020b) defines drought as rainfall in the lowest decile (i.e., below the tenth percentile) of historical totals, and we adopt their definition in our analysis. Within each lowest decile year,

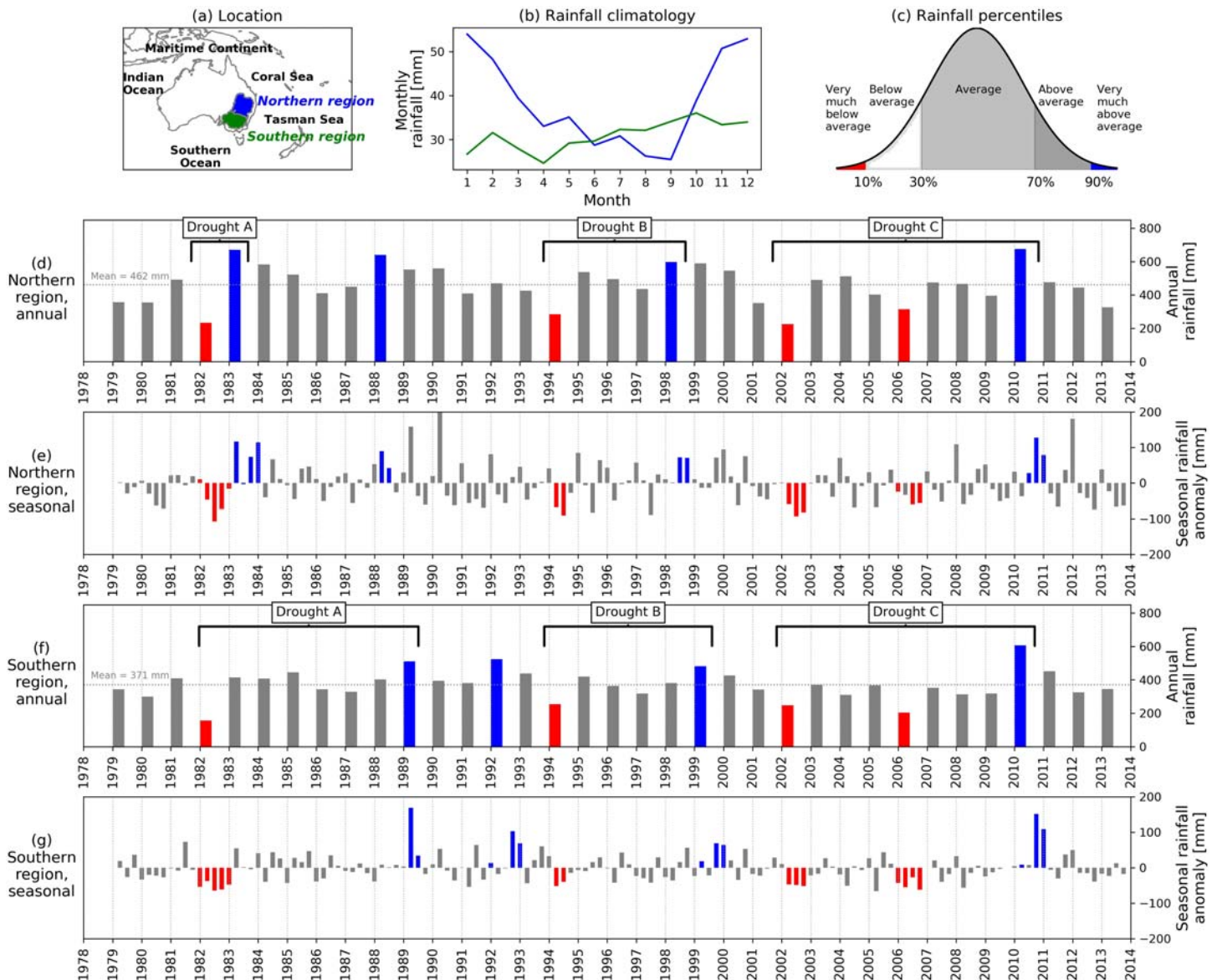


Figure 1. Timeseries of droughts. (a) Location of regions and oceans set within the model domain; (b) rainfall climatology; (c) definition of rainfall percentiles; (d) annual rainfall with mean; and (e) seasonal rainfall anomalies in the northern region; (f) and (g) as (d) and (e) but for the southern region. Years with annual rainfall in the lowest decile and their corresponding seasons with below-average rainfall are marked in red; years in the top decile and their corresponding above-average seasons are marked in blue.

drought seasons are those where the seasonal rainfall was below average (Figure 1c). Drought onset is taken as the first season of drought, with the remaining seasons considered as the drought intensification stage. Drought terminating years are those in the highest decile (i.e., above the 90th percentile). Within terminating years, drought termination seasons are those where the seasonal rainfall was above average (Figure 1c). Based on these definitions, three drought periods occurred starting in 1982 (Drought A), 1994 (Drought B), and 2002 (Drought C). The droughts terminated in different years between the regions, except for Drought C, which terminated in 2010 (Figure 1).

We also estimated drought stages using the Standardized Precipitation Index (SPI, McKee et al., 1993; see supporting information). Results were very similar using the SPI, and therefore, we focus on the percentile-based drought definition. The definitions of drought used rainfall estimated from the WRFv3.6.1 simulation for 1979–2013, to remain consistent with the back-trajectory analysis.

2.3. Estimating Amplification

The degree to which local land-atmosphere feedbacks affected each drought stage was assessed via the rainfall recycling ratio (P_R). The 3-D time series of evaporative origin, obtained with the back-trajectory analysis, was used to calculate the proportion of rainfall in a region A (P_A), whose moisture was derived from evapotranspiration within the same region (M_L): $P_R = M_L/P_A[\%]$. To identify whether land surface processes amplified or dampened rainfall anomalies during drought, we examined the change in the local terrestrial moisture contribution compared to the rainfall anomaly. The anomalies were calculated from the region's seasonal rainfall climatology. For rainfall in a region on any given day, we retained full spatial information on the origin of the precipitated moisture through the back-trajectory results. We calculated an amplification factor (A_L), expressed as follows:

$$A_L = \frac{\Delta M_L}{\Delta P}$$

where ΔM_L (mm) is the anomaly in the contribution of moisture from the local land surface to rainfall and ΔP (mm) is the total anomaly in rainfall. Similarly, we estimated amplification factors for the moisture contributions from the nonlocal land surface (A_{NL}) and the ocean (A_O).

3. Results

3.1. Source Region Change During Drought

Drought onset in the northern (Figures 2a–2d) and southern (Figures 3a–3d) regions was dominated by reduced marine moisture from the Tasman and Coral Seas to the east of Australia (Figure 1a), with low-level winds directing moist marine air away from each region more often than normal (Figure S1). Drought onset was typically associated with reduced terrestrial moisture from the land surface. For the northern region this was within and directly north of the basin. For the southern region, terrestrial anomalies consistently originated from within the northern region.

Drought intensification was also dominated by reduced marine moisture from the Tasman and Coral Seas but covered a larger geographical extent than the onset stage, extending to the subtropical Indian and Southern Oceans (Figures 2e–2h and 3e–3h). For the northern region, terrestrial anomalies remained similar in spatial extent and intensity to those for the onset stage. For the southern region, the spatial extent of terrestrial anomalies increased as droughts intensified from initially the northern region only, to eventually include both regions.

Drought termination in both regions was consistently associated with above-average moisture contribution from the Coral and Tasman Seas, in line with strengthened easterly flow (Figures 2i–2l and 3i–3l) compared to the seasonal expectation (Figure S1). Drought-breaking marine moisture anomalies were similar in spatial extent between events (especially for the northern region), extending from approximately 20 to 30°S and east of the continent to approximately 160°E. Drought-breaking marine moisture contributions were from a larger area for the southern region, encompassing the Tasman Sea and Southern Ocean, but with marine moisture anomalies from the Tasman Sea contributing most strongly to termination. Positive anomalies in moisture supply from terrestrial sources were consistent between termination events and mirrored the negative terrestrial anomalies identified during the intensification stage for both regions.

3.2. Moisture Supply and Rainfall Favorability

To determine whether the anomalously low moisture contribution during drought was due to a reduction in evaporation in the main marine source regions or due to redirection of the moisture elsewhere, we evaluated several hydrometeorological metrics for each drought and compared them to their values for subsequent termination stages (Figure 4). The difference in rainfall during drought years and their respective termination years in the northern region is evident in cumulative rainfall (Figures 4a–4c). For the northern region, the low rainfall during drought years was not due to a reduction in evaporation in the marine source regions (marine evaporation differed little between drought and termination years; Figures 4d–4f). A similar amount of total precipitable water (TPW) was available during the drought year A (1982) and its termination (1983; Figure 4g). In drought year B (1994), the TPW fell below 1998 values in the second half of the year (Figure 4h). For both droughts A and B the 500 hPa maximum vertical wind speed suggests large-scale

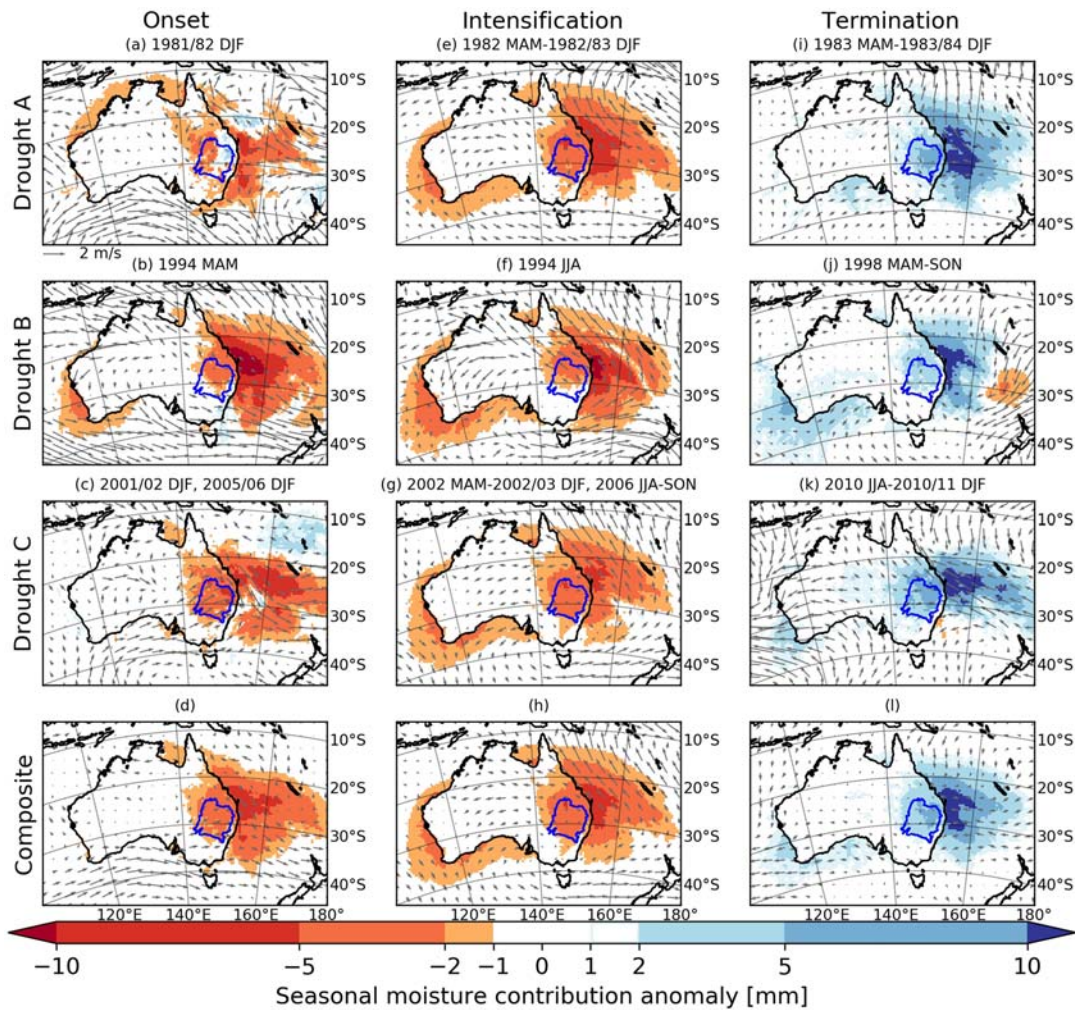


Figure 2. Moisture source anomalies during drought (a–d) onset, (e–h) intensification, and (i–l) termination in the northern region overlain by low-level wind speed anomalies. Droughts A, B, and C are represented in the top three rows, with the bottom row showing their mean.

uplift was greater in the termination year, particularly from April to November (Figures 4j and 4k). This suggests that even if the amount of atmospheric moisture was similar in the drought and termination years of Drought A (and in the first half of Drought B), there was a lack of mechanisms to generate precipitation. In Drought C (the Millennium Drought), both TPW (Figure 4i) and vertical uplift (Figure 4l) were lower than the termination year (2010).

Low rainfall in the southern region could also not be attributed to a reduction in evaporation in the marine source regions (Figures 4d–4f). However, in contrast to the northern region, no consistent difference in precipitation favorability was suggested by vertical wind speed for Droughts A–C (Figures 4j–4l). Instead, during the three droughts, there was an apparent lack of TPW compared to the termination years (Figures 4g–4i).

3.3. Amplification of Drought Stages

In all stages of drought, the local land surface amplified the rainfall anomaly to a similar degree in the northern ($A_L = 5.1\text{--}6\%$) and southern ($3.1\text{--}4.5\%$; Table 1c) regions of the MDB. In the northern region, the local land played a larger role than normal during anomalous rainfall periods: It amplified the negative rainfall anomaly during drought onset and intensification and amplified the positive rainfall anomaly during drought termination (Table 1c). In the southern region local land amplification was limited during each drought stage compared to climatology.

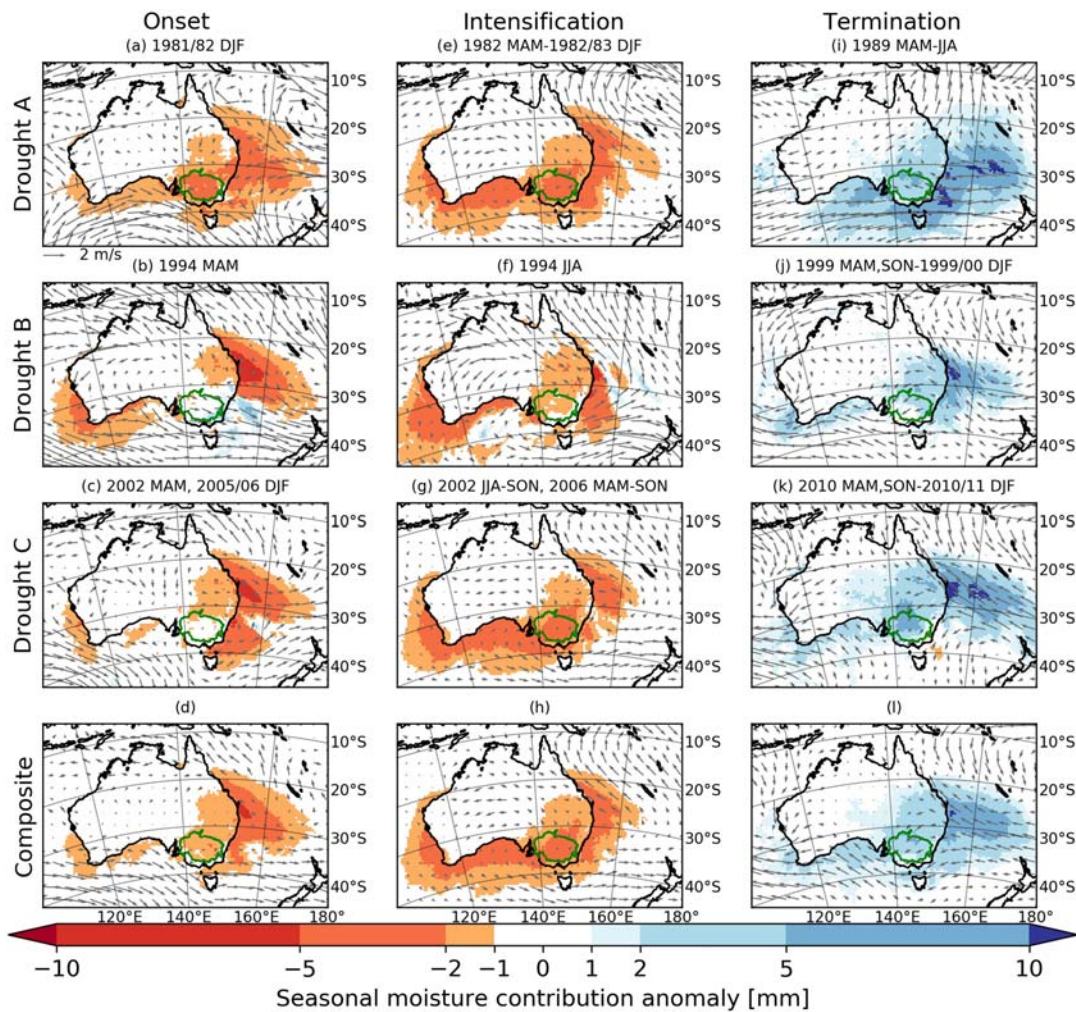


Figure 3. As for Figure 2 but for the southern region.

Rainfall anomalies during drought and termination were also amplified by the ocean and the nonlocal land surface. Rainfall in both basins was most influenced by the ocean ($A_O > 73.9\%$; Table 1c). Land-atmosphere feedbacks, as estimated by rainfall recycling, played a comparatively stronger role in amplifying rainfall anomalies in the northern region (6.4%, 4.8%, and 5.3% during onset, intensification, and termination, respectively) than the southern region (4%, 2.8%, and 3.9% during onset, intensification, and termination, respectively). Comparatively stronger land-atmosphere feedbacks were expected in the northern region compared to the south (Table 1; Figures S1i and S1j).

4. Discussion

Rainfall over the MDB is associated with different synoptic types (e.g., Pook et al., 2006) influenced by large-scale drivers including the El Niño-Southern Oscillation, Indian Ocean Dipole, Southern Annular Mode, and atmospheric blocking (Risbey et al., 2009; Verdon-Kidd & Kiem, 2009). These large-scale modes influence the weather systems during drought and likely also affect the typical sources of moisture. Here, a Lagrangian back-trajectory approach was used to identify changes to moisture supply during major droughts in the MDB. Our results demonstrate the importance of moisture advection during drought and therefore emphasize the need to characterize the relationship between moisture sources and synoptic-scale processes and how the relationship is modified by broader-scale circulation changes. More broadly, our results highlight the importance of understanding the relationship between moisture advection and atmospheric

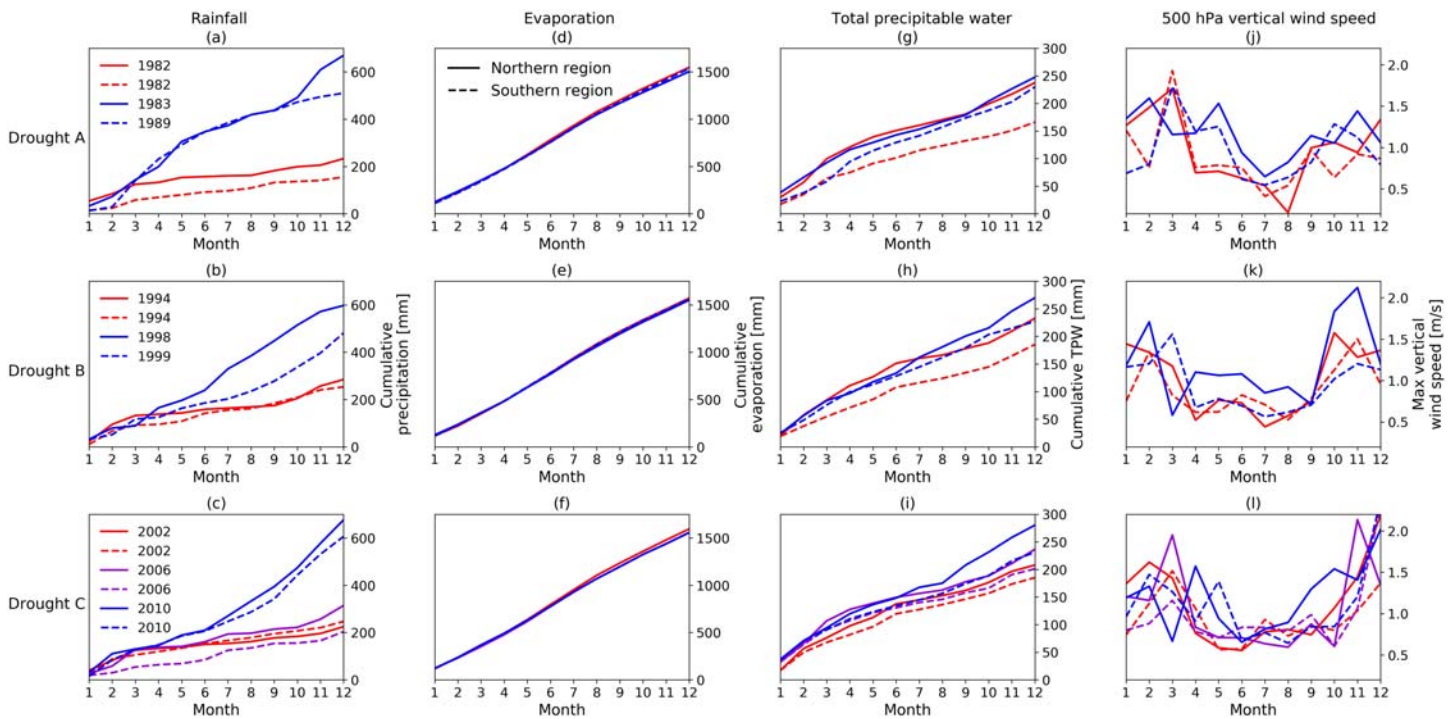


Figure 4. Plots of cumulative monthly (a–c) rainfall, (d–f) marine evaporation, (g–i) total precipitable water, and (j–l) 500 hPa maximum vertical wind speed for Droughts A–C in the northern (solid lines) and southern regions (dashed lines). Drought years are indicated by red/purple lines, termination years by blue lines.

circulation in regions where, like southeast Australia, rainfall is subject to large-scale modes of variability, including parts of the United States, South America, Asia, and Africa.

Our results show that anomalous atmospheric circulation modified the strength of moisture advection from key moisture sources during each drought stage. Climatologically, moist easterlies contribute to year-round rainfall in the MDB and are supplemented by moist westerlies in winter and spring (Figure S1). During drought, anticyclonic conditions over the MDB directed the typical easterly flow of moisture toward the northwest and the typical westerly flow toward the southeast, depriving the basin of moisture (Figures 2 and 3). In contrast, during drought termination moist easterly advection strengthened, bringing enhanced marine moisture for rainfall. Our results are therefore consistent with Rakich et al. (2008) and Pepler et al. (2016) who demonstrated a clear relationship between strong easterlies and higher summer rainfall across southeast Australia and weakened easterlies with lower rainfall. In winter, stronger westerlies were associated with wetter conditions in the southern part of southeastern Australia (Pepler et al., 2016). There is, therefore, a need to investigate the impact of synoptic systems on the relationship between zonal winds, moisture advection, and rainfall during southeast Australian droughts.

In addition to a reduction in advected marine moisture, the land surface also contributed to drought intensification. Drought in the northern region was exacerbated by a reduction in precipitation-generating mechanisms. This may be due to a reduction in local convective activity, suggested by the reduction in rainfall recycling and amplification of dry conditions by the local land surface during drought intensification. In the southern region, the local land surface exacerbated dry conditions but to a smaller degree than normal. In contrast, the typically large role played by ocean moisture in amplifying anomalous rainfall was further enhanced during drought. The suppression of the local land's usual role in generating rainfall and the enhanced role of the ocean both indicate that the ocean and remote processes became an even stronger driver of rainfall anomalies in the southern region during drought.

The nonlocal land surface amplified southern region rainfall anomalies during drought more than local processes. The nonlocal land surface, including the northern part of the MDB, amplified southern

Table 1
Amplification Factors A Expressed as a Percentage for (a) Seasonal Climatology, (b) Seasons Comprising Drought Stages, and (c) During Drought Stages

	(a) Climatology (%)				(b) Climatological expectation (%)				(c) A (%)		
	Summer	Autumn	Winter	Spring	Onset	Intensification	Termination	Onset	Intensification	Termination	
Northern region											
Local land (A_L)	4.4	0.5	3.3	8.6	3.4	4.4	4.6	6.0	5.7	5.1	
Nonlocal land (A_{NL}), total	25.4	12.0	8.8	13.3	22.0	13.6	14.1	16.9	17.3	12.7	
Ocean (A_O)	72.1	87.4	87.5	78.4	75.9	82.2	81.7	76.5	76.4	82.2	
Local land (A_L)	4.9	3.0	2.0	13.5	4.0	5.9	6.0	3.1	4.5	4.1	
Nonlocal land (A_{NL}), total	35.3	22.7	11.4	39.8	29.0	24.6	28.7	17.3	18.3	21.7	
Nonlocal land (A_{NL}), northern region component	6.8	2.5	2.9	6.4	4.7	4.3	4.6	3.9	3.9	4.8	
Ocean (A_O)	58.9	73.1	86.4	47.2	66.0	69.2	64.8	79.0	76.8	73.9	

Note. Values in (c) are bold where they exceed the climatological expectation in (b) and italicized where they are below the climatological expectation. Total amplification (i.e., $A_L + A_{NL} + A_O$) does not add to exactly 100% due to model discrepancy (<2%) between the amount of simulated rainfall and amount of moisture back-tracked.

region rainfall anomalies, especially during drought termination. This means the southern region is partly reliant on moisture advected from the northern region for droughts to terminate and is more vulnerable to land use changes that alter evapotranspiration and thus the supply of moisture for rainfall (Pitman et al., 2004). While past studies have found that land cover changes have increased the severity of droughts in southeast Australia (Mcalpine et al., 2009), our analysis indicates that land use and land cover changes in the northern region would have an impact on the supply of atmospheric moisture for rainfall in the southern region. Our results, therefore, highlight a potential mechanism to partly explain declines in rainfall over the southern MDB that requires further investigation.

There are some limitations to our approach. We used a single modeling system—WRFv3.6.1 driven with ERA-Interim reanalyses—together with a Lagrangian back-trajectory algorithm. While WRFv3.6.1 has been shown to work well over southeast Australia when using ERA-Interim (Di Virgilio et al., 2019), and uncertainties in the back-trajectory model are likely to have only a small impact on results (Holgate et al., 2020), we cannot discount that our results are partly dependent on this choice of modeling system.

Simulating droughts in southeast Australia has been an ongoing challenge (Ukkola et al., 2018). Modes of variability, global warming, ozone depletion, sea ice dynamics, land use, and land cover change have all been proposed as partial explanations for drought. Our back-trajectory approach demonstrates that to simulate droughts for the right physical reasons, models need to source moisture from the right marine and terrestrial regions and in the right proportions. Our analysis also suggests that the initiation of droughts, their intensification, and termination have distinct signatures. A climate model used to simulate droughts should match these signatures, which are established by interactions between the modes of variability, in a warming climate, and moderated or ameliorated by land surface feedbacks. This places a considerable demand on climate models, but where models fail to capture these signatures, at least acknowledging these current shortcomings guides where future improvements need to take place.

5. Conclusion

We have shown that major southeast Australian droughts were intensified and terminated chiefly by anomalies of marine moisture from the Tasman and Coral Seas associated with shifts in atmospheric circulation. During drought, anomalous atmospheric circulation patterns redirected moisture away from southeast Australia. This reversed during drought termination, promoting strong advection of moisture from the ocean into the region. This highlights the need to prioritize understanding of the relationship between synoptic-scale circulation and moisture advection, and how this relationship is modified by large-scale climate variability, in drought-prone regions of the world.

While a reduction in advected marine moisture was the dominant cause of drought throughout the MDB, the northern region also experienced a reduction in conditions favorable for the precipitation of available atmospheric moisture. This highlights the need to identify the mechanisms responsible for the suppression of rainfall generation during drought and specifically whether these mechanisms reflect local convective or larger-scale rainfall generating mechanisms.

We showed the land surface acted to amplify rainfall anomalies during all stages of drought. Local terrestrial moisture played a secondary role to ocean moisture contributions which dominated the development and termination of drought in southeast Australia. However, we found evidence that reduced moisture sources in the

northern region might partly explain reductions in rainfall in the southern region, a result that deserves further exploration.

The physical mechanisms leading to drought and its termination shown by our results provide a template for evaluating climate models used for simulating droughts. A research priority is to examine whether any of the current generation of climate models simulate droughts over southeast Australia with signatures and a relative role of marine and terrestrial moisture sources that are in line with the mechanisms we identified. More broadly, our approach provides a framework for investigating causal mechanisms of drought that can be applied to other regions of the world.

Data Availability Statement

CORDEX-Australasia climate simulations used in this study are publicly available (<https://climatedata.environment.nsw.gov.au/>).

Acknowledgments

This work was possible thanks to an Australian National University AGRT Scholarship (C.M.H.) and support from the ARC Centre of Excellence for Climate System Science (CE110001028). C.M.H. and A.I.J.M.v.D. were supported through the ARC Discovery Projects funding scheme (project DP40103679). J.P.E. and A.J.P. were supported via the ARC Centre of Excellence for Climate Extremes (CE170100023). The authors thank the staff at NCI, A. Ukkola, G. di Virgilio, D. Miralles, and R. Van Der Ent.

References

- Ashok, K., Guan, Z., & Yamagata, T. (2003). Influence of the Indian Ocean Dipole on the Australian winter rainfall. *Geophysical Research Letters*, *30*(15), 1821. <https://doi.org/10.1029/2003GL017926>
- Boer, M. M., de Dios, V. R., & Bradstock, R. A. (2020). Unprecedented burn area of Australian mega forest fires. *Nature Climate Change*, *10*(3), 171–172. <https://doi.org/10.1038/s41558-020-0716-1>
- Bosilovich, M. G., & Chern, J.-D. (2006). Simulation of water sources and precipitation recycling for the MacKenzie, Mississippi, and Amazon River Basins. *Journal of Hydrometeorology*, *7*(3), 312–329. <https://doi.org/10.1175/JHM501.1>
- Bureau of Meteorology. (2020a). Annual Australian Climate Statement 2019. Retrieved April 6, 2020, from <http://www.bom.gov.au/climate/current/annual/aus/#tabs=Events>
- Bureau of Meteorology. (2020b). What is drought? Retrieved March 12, 2020, from <http://www.bom.gov.au/climate/drought/knowledge-centre/understanding.shtml>
- Chiew, F. H. S., Piechota, T. C., Dracup, J. A., & McMahon, T. A. (1998). El Niño/Southern Oscillation and Australian rainfall, streamflow and drought: Links and potential for forecasting. *Journal of Hydrology*, *204*(1–4), 138–149. [https://doi.org/10.1016/S0022-1694\(97\)00121-2](https://doi.org/10.1016/S0022-1694(97)00121-2)
- Di Virgilio, G., Evans, J. P., Di Luca, A., Olson, R., Argüeso, D., Kala, J., et al. (2019). Evaluating reanalysis-driven CORDEX regional climate models over Australia: Model performance and errors. *Climate Dynamics*, *53*(5–6), 2985–3005. <https://doi.org/10.1007/s00382-019-04672-w>
- Dirmeyer, P. A., & Brubaker, K. L. (1999). Contrasting evaporative moisture sources during the drought of 1988 and the flood of 1993. *Journal of Geophysical Research*, *104*(D16), 19,383–19,397. <https://doi.org/10.1029/1999JD900222>
- Drumond, A., Gimeno, L., Nieto, R., Trigo, R. M., & Vicente-Serrano, S. M. (2017). Drought episodes in the climatological sinks of the Mediterranean moisture source: The role of moisture transport. *Global and Planetary Change*, *151*, 4–14. <https://doi.org/10.1016/j.gloplacha.2016.12.004>
- Gimeno, L., Drumond, A., Nieto, R., Trigo, R. M., & Stohl, A. (2010). On the origin of continental precipitation. *Geophysical Research Letters*, *37*, L13804. <https://doi.org/10.1029/2010GL043712>
- Hendon, H. H., Thompson, D. W. J., & Wheeler, M. C. (2007). Australian rainfall and surface temperature variations associated with the Southern Hemisphere annular mode. *Journal of Climate*, *20*(11), 2452–2467. <https://doi.org/10.1175/JCLI4134.1>
- Herrera-Estrada, J. E., Martinez, J. A., Dominguez, F., Findell, K. L., Wood, E. F., & Sheffield, J. (2019). Reduced moisture transport linked to drought propagation across North America. *Geophysical Research Letters*, *46*, 5243–5253. <https://doi.org/10.1029/2019GL082475>
- Holgate, C. M., Evans, J. P., Van Dijk, A. I. J. M., & Pitman, A. J. (2020). Australian precipitation recycling and evaporative source regions. *Journal of Climate*, 1–40. <https://doi.org/10.1175/JCLI-D-19-0926.1>
- Hughes, N., Galeano, D., & Hatfield-Dodds, S. (2019). The effects of drought and climate variability on Australian farms. In *Australian bureau of agricultural and resource economics and sciences* (Vol. 6, p. 11). Canberra: Australian Bureau of Agricultural and Resource Economics and Sciences. <https://doi.org/10.25814/5de84714f6e08>
- Mcalpine, C. A., Syktus, J., Ryan, J. G., Deo, R. C., Mckee, G. M., MCGowan, H. A., & Phinn, S. R. (2009). A continent under stress: Interactions, feedbacks and risks associated with impact of modified land cover on Australia's climate. *Global Change Biology*, *15*(9), 2206–2223. <https://doi.org/10.1111/j.1365-2486.2009.01939.x>
- McKee, T. B., Doesken, N. J., & Kleist, J. (1993). The relationship of drought frequency and duration to time scales. In *Proceedings of the 8th Conference of Applied Climatology, 17–22 January*. Anaheim, CA: American Meteorological Society. Retrieved from <https://pdfs.semanticscholar.org/c3f7/136d6cb726b295eb34565a8270177c57f40f.pdf>
- Miralles, D. G., Nieto, R., McDowell, N. G., Dorigo, W. A., Verhoest, N. E., Liu, Y. Y., et al. (2016). Contribution of water-limited ecoregions to their own supply of rainfall. *Environmental Research Letters*, *11*(12), 124007. <https://doi.org/10.1088/1748-9326/11/12/124007>
- Murray-Darling Basin Authority. (2020). Water in storages. Retrieved March 12, 2020, from <https://www.mdba.gov.au/managing-water/water-storage>
- Pepler, A. S., Alexander, L. V., Evans, J. P., & Sherwood, S. C. (2016). Zonal winds and southeast Australian rainfall in global and regional climate models. *Climate Dynamics*, *46*(1–2), 123–133. <https://doi.org/10.1007/s00382-015-2573-6>
- Pitman, A. J., Narisma, G. T., Pielke, R. A., & Holbrook, N. J. (2004). Impact of land cover change on the climate of southwest Western Australia. *Journal of Geophysical Research*, *109*, D18109. <https://doi.org/10.1029/2003JD004347>
- Pook, M. J., McIntosh, P. C., & Meyers, G. A. (2006). The synoptic decomposition of cool-season rainfall in the Southeastern Australian cropping region. *Journal of Applied Meteorology and Climatology*, *45*(8), 1156–1170. <https://doi.org/10.1175/JAM2394.1>
- Power, S., Casey, T., Folland, C., Colman, A., & Mehta, V. (1999). Inter-decadal modulation of the impact of ENSO on Australia. *Climate Dynamics*, *15*(5), 319–324. <https://doi.org/10.1007/s003820050284>

- Rakich, C. S., Holbrook, N. J., & Timbal, B. (2008). A pressure gradient metric capturing planetary-scale influences on eastern Australian rainfall. *Geophysical Research Letters*, *35*, L08713. <https://doi.org/10.1029/2007GL032970>
- Risbey, J. S., Pook, M. J., McIntosh, P. C., Wheeler, M. C., & Hendon, H. H. (2009). On the remote drivers of rainfall variability in Australia. *Monthly Weather Review*, *137*(10), 3233–3253. <https://doi.org/10.1175/2009MWR2861.1>
- Roundy, J. K., Ferguson, C. R., & Wood, E. F. (2013). Temporal variability of land–atmosphere coupling and its implications for drought over the Southeast United States. *Journal of Hydrometeorology*, *14*(2), 622–635. <https://doi.org/10.1175/JHM-D-12-090.1>
- Roy, T., Martinez, J. A., Herrera-Estrada, J. E., Zhang, Y., Dominguez, F., Berg, A., et al. (2019). Role of moisture transport and recycling in characterizing droughts: Perspectives from two recent U.S. droughts and the CFSv2 system. *Journal of Hydrometeorology*, *20*(1), 139–154. <https://doi.org/10.1175/JHM-D-18-0159.1>
- Schubert, S. D., Stewart, R. E., Wang, H., Barlow, M., Berbery, E. H., Cai, W., et al. (2016). Global meteorological drought: A synthesis of current understanding with a focus on SST drivers of precipitation deficits. *Journal of Climate*, *29*(11), 3989–4019. <https://doi.org/10.1175/JCLI-D-15-0452.1>
- Stojanovic, M., Drumond, A., Nieto, R., & Gimeno, L. (2017). Moisture transport anomalies over the Danube River basin during two drought events: A Lagrangian analysis. *Atmosphere*, *8*(12), 193. <https://doi.org/10.3390/atmos8100193>
- Ukkola, A. M., Pitman, A. J., De Kauwe, M. G., Abramowitz, G., Herger, N., Evans, J. P., & Decker, M. (2018). Evaluating CMIP5 model agreement for multiple drought metrics. *Journal of Hydrometeorology*, *19*(6), 969–988. <https://doi.org/10.1175/JHM-D-17-0099.1>
- Ummenhofer, C. C., Sen Gupta, A., Briggs, P. R., England, M. H., McIntosh, P. C., Meyers, G. A., et al. (2010). Indian and Pacific Ocean influences on southeast Australian drought and soil moisture. *Journal of Climate*, *24*(5), 1313–1336. <https://doi.org/10.1175/2010JCLI3475.1>
- Van Der Ent, R. J., Savenije, H. H. G., Schaefli, B., & Steele-Dunne, S. C. (2010). Origin and fate of atmospheric moisture over continents. *Water Resources Research*, *46*, W09525. <https://doi.org/10.1029/2010WR009127>
- Van Dijk, A. I. J. M., Beck, H. E., Crosbie, R. S., de Jeu, R. A. M., Liu, Y. Y., Podger, G. M., et al. (2013). The millennium drought in Southeast Australia (2001–2009): Natural and human causes and implications for water resources, ecosystems, economy, and society. *Water Resources Research*, *49*, 1040–1057. <https://doi.org/10.1002/wrcr.20123>
- Verdon-Kidd, D. C., & Kiem, A. S. (2009). On the relationship between large-scale climate modes and regional synoptic patterns that drive Victorian rainfall. *Hydrology and Earth System Sciences*, *13*(4), 467–479. <https://doi.org/10.5194/hess-13-467-2009>
- Wei, J., Jin, Q., Yang, Z.-L., & Dirmeyer, P. A. (2016). Role of Ocean Evaporation in California Droughts and Floods. *Geophysical Research Letters*, *43*, 6554–6562. <https://doi.org/10.1002/2016GL069386>
- Yu, P., Xu, R., Abramson, M. J., Li, S., & Guo, Y. (2020). Bushfires in Australia: A serious health emergency under climate change. *The Lancet Planetary Health*, *4*(1), e7–e8. [https://doi.org/10.1016/S2542-5196\(19\)30267-0](https://doi.org/10.1016/S2542-5196(19)30267-0)
- Zeng, D., Yuan, X., & Roundy, J. K. (2019). Effect of Teleconnected land–atmosphere coupling on Northeast China persistent drought in spring–summer of 2017. *Journal of Climate*, *32*(21), 7403–7420. <https://doi.org/10.1175/JCLI-D-19-0175.1>
- Zhou, S., Williams, A. P., Berg, A. M., Cook, B. I., Zhang, Y., Hagemann, S., et al. (2019). Land–atmosphere feedbacks exacerbate concurrent soil drought and atmospheric aridity. *Proceedings of the National Academy of Sciences*, *116*(38), 18,848–18,853. <https://doi.org/10.1073/pnas.1904955116>